PROCEEDINGS OF SCIENCE

Spin Physics @ FAIR

Marco Destefanis[*†]
Università degli Studi di Torino, Italy, and INFN
E-mail: destefan@to.infn.it

Our knowledge on the nucleonic structure is still uncomplete. A transverse momentum dependent description of the nucleon structure is a crucial milestone of several forthcoming studies in a wide range of experimental scenarios. The physics program of the future FAIR facility includes the investigation of the nucleon structure by mean of antiproton beams, eventually polarised, with a beam momentum up to 15 GeV/c, in kinematic regions where perturbative QCD could not yet completely hold. The Drell-Yan production of lepton pairs in antiproton-proton scattering is a uniqe tool to access the spin depending properties of the nucleon, and in particular its transverse degrees of freedom, by mean of experimental asymmetries leading to Transverse Momentum Dependent (TMD) Parton Distribution Functions (PDF's). The spin physics program that could be accomplished at FAIR, and in particular by mean of the PANDA spectrometer, will be discussed in details.

XLIX International Winter Meeting on Nuclear Physics
24-28 January 2011
BORMIO, Italy

[*]Speaker.
[†]On behalf of the PANDA Collaboration.

PoS(Bormio 2011)012

1. Motivation

The complete description of the nucleonic structure requires both the parton distribution functions (PDF) and the fragmentation functions (FF). At the leading twist three PDF's are needed to describe the quark structure of a hadron: the unpolarized function $f_1(x)$, the longitudinal polarization distribution $g_1(x)$, and the transverse polarization $h_1(x)$. The $f_1(x)$ function describes the probability of finding a quark with a fraction x of the longitudinal momentum of the parent hadron regardless on the quark's spin orientation; the $g_1(x)$ function is the helicity distribution of the quarks; the $h_1(x)$ function, a.k.a. Transversity, describes the quarks' transverse spin distribution inside a transversely polarized hadron. Transversity has no probabilistic interpretation in the helicity basis; moreover it is chirally odd and hence it could not be extracted from the historical deep inelastic scattering (DIS) data [1].

The difficult interpretation of the experimental polarized cross sections in high energy hadron-hadron scattering suggests that other factors have to be taken into account [2]. In the last decade many efforts were devoted to understand the role of the intrinsic transverse momentum of the partons ($\mathbf{k}_T$). A full set of Transverse Momentum Dependent (TMD) PDF and FF was introduced. In order to obtain a complete description of the nucleonic structure in a leading twist TMD approach, the three PDF's above described are no more enough, and eight independent PDF's, functions of x and $\mathbf{k}_T$, are needed. Fig. 1 shows such eight TMD PDF's: f_1, g_{1L}, $f_{1T}^{\perp}$, and g_{1T} are chirally even functions, while $h_1^{\perp}$, $h_{1L}^{\perp}$, h_{1T}, and $h_{1T}^{\perp}$ are chirally odd.

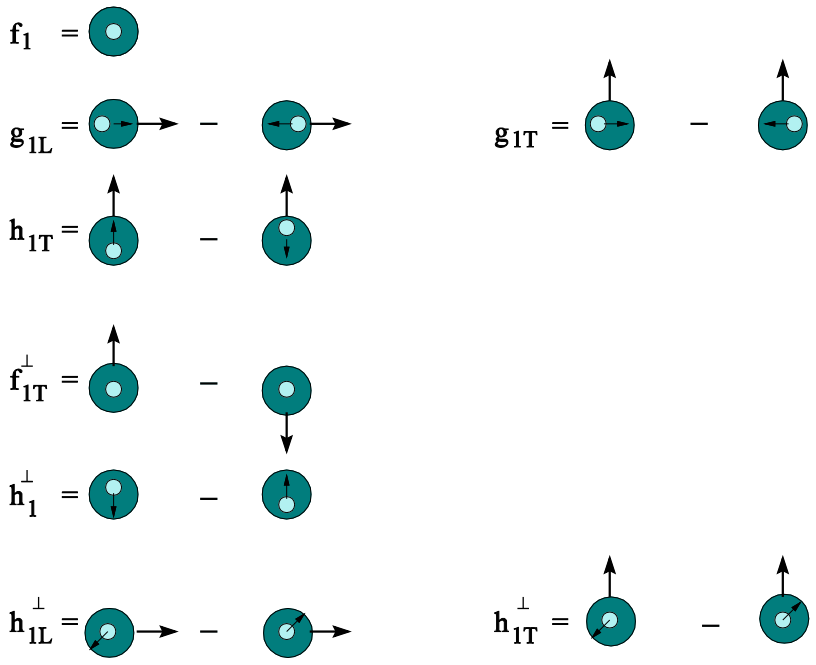

Figure 1: *TMD PDF's distributions. The arrows indicate the polarizations of the quark and of the parent hadron.*

The TMD PDF's can be investigated in different experimental scenarios. Semi-Inclusive Deep Inelastic Scattering (SIDIS) experiments are currently allowing to probe the hadron structure at

different energies, and with different beam-target configurations. But in such cases, the TMD PDF's can be extracted only from their convolution with other FF, posing hence experimental and theoretical challenges to their extraction. On the contrary the Drell-Yan (DY) production of lepton pairs allows to directly access TMD PDF's, since in such scenarios one can define experimental asymmetries depending on the TMD PDF's only. In the considered DY process a quark-antiquark annihilation proceeds through a virtual photon into a final state containing a lepton pair: $h_1 h_2 \rightarrow l^+ l^- X$. The usually adopted Collins-Soper frame [3] (shown in Fig. 2) is defined considering the lepton's production plane. Another relevant plane is that containing the annihilating quark-

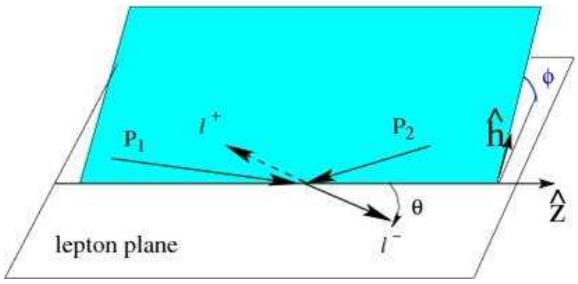

Figure 2: *Virtual photon rest frame, so called Collins-Soper frame.*

antiquark momenta; φ is than the angle defined by the two planes, and $\varphi_{S_{1,2}}$ the angle of the nucleon spin ($S_{1,2}$) with respect to the lepton plane.

DY processes allow as well for an effective test of QCD Universality. The $f_{1T}^{\perp}$ function (a.k.a. Sivers function) deduced from the SIDIS data is expected to be opposite with respect to that extracted from DY data:

$$f_{1T}^{\perp}|_{SIDIS} = -f_{1T}^{\perp}|_{DY}. \tag{1.1}$$

The asymmetry corresponding to $f_{1T}^{\perp}$ [4] could be observed convoluted with another time-reversal odd function. Considering a deep inelastic processes and applying the factorization theorem, the parton density can be defined as the elementary fields multiplied by the Wilson lines [5]:

$$P(x,\mathbf{k}_T,\mathbf{s}_T,\zeta) = \int \frac{dy^- d^2\mathbf{y}_T}{(2\pi)^3} e^{-ixp^+y^- + i\mathbf{k}_T\mathbf{y}_T} \times < p|\bar{\psi}(0,y^-,\mathbf{y}_T) W_{y\infty}^{\dagger} \frac{\gamma^+}{2} W_{0\infty}\psi(0)|p>, \tag{1.2}$$

where x and $\mathbf{k}_T$ indicate the fraction of the longitudinal and transverse momentum, respectively, carried by the quark; the transverse part of the hadron spin vector is $\mathbf{s}_T$; in light-front coordinates $y^\mu = (y^+,y^-,\mathbf{y}_T) = ((y^0 \pm y^z)/\sqrt{2},\mathbf{y}_T)$. The variable ζ is associated to the direction of the Wilson-line operator (W). The Wilson-line ensure the colour gauge invariance, and $W_{y\infty}$ indicates a Wilson-line operator which goes from the point y to future infinity, which means that those lines are going in the light-like direction. When applying space- and time-reversal to the parton density operator of eq. 1.2 one has to take into account also the Wilson-lines, so the future-pointing direction is replaced by the past-pointing direction:

$$P(x,\mathbf{k}_T,\mathbf{s}_T,\zeta)|_{future-pointing\ W} = -P(x,\mathbf{k}_T,-\mathbf{s}_T,\zeta)|_{past-pointing\ W}. \tag{1.3}$$

The DY process can be factorized by the past-pointing Wilson-lines, so the Sivers asymmetry, which depends on x, $\mathbf{k}_T$, and ζ, has opposite sign for SIDIS and DY, leading to eq. 1.1.

The differential cross section of the completely unpolarised DY process can be expressed as:

$$\frac{d\sigma^0}{d\Omega dx_1 dx_2 dq_T} = \frac{\alpha^2}{12Q^2}\sum_f e_f^2 \Bigg\{ (1+\cos^2\vartheta) F\left[\bar{f}_1^f f_1^f\right] + \\ + f\sin^2\vartheta\cos 2\varphi F\left[\left(2\hat{\mathbf{h}}\cdot\mathbf{p}_{1_T}\hat{\mathbf{h}}\cdot\mathbf{p}_{2_T} - \mathbf{p}_{1_T}\cdot\mathbf{p}_{2_T}\right)\frac{\bar{h}_1^{\perp f} h_1^{\perp f}}{M_1 M_2}\right]\Bigg\}, \tag{1.4}$$

where α is the fine structure constant, e_f is the charge of a parton with flavour f, and q_T is the transverse momentum of the lepton pair. $h_1^\perp$ is the so called Boer-Mulders (BM) function, which describes the distribution of the transversely polarised quarks in an unpolarised hadron. In a TMD approach, a $\cos(2\varphi)$ azimuthal dependence contributes hence to the leading twist description of the cross section; the corresponding TMD $h_1^\perp$ is a function that can be connected to the orbital motion of the parton inside the hadron.

In the single-polarised case, in which one of the annihilating hadrons is transversely polarised, a further term contributes at leading twist to the differential cross section:

$$\frac{d\sigma}{d\Omega dx_1 dx_2 dq_T} = \frac{d\sigma^0}{d\Omega dx_1 dx_2 dq_T} + \frac{d\Delta\sigma^\uparrow}{d\Omega dx_1 dx_2 dq_T}, \tag{1.5}$$

where

$$\frac{d\Delta\sigma^\uparrow}{d\Omega dx_1 dx_2 dq_T} = \frac{\alpha^2}{12sQ^2}\sum_f e_f^2 |\mathbf{S}_{2_T}| \Bigg\{ (1+\cos^2\vartheta)\sin(\varphi-\varphi_{S_2}) F\left[\hat{\mathbf{h}}\cdot\mathbf{p}_{2_T}\frac{\bar{f}_1^f f_{1T}^{\perp f}}{M_2}\right] + \\ -\sin^2\vartheta\sin(\varphi+\varphi_{S_2}) F\left[\hat{\mathbf{h}}\cdot\mathbf{p}_{1_T}\frac{\bar{h}_1^\perp h_{1T}^f}{M_1}\right] + \\ -\sin^2\vartheta\sin(3\varphi-\varphi_{S_2}) F\left[\left(4\hat{\mathbf{h}}\cdot\mathbf{p}_{1_T}(\hat{\mathbf{h}}\cdot\mathbf{p}_{2_T})^2 - 2\hat{\mathbf{h}}\cdot\mathbf{p}_{2_T}\mathbf{p}_{1_T}\cdot\mathbf{p}_{2_T} - \hat{\mathbf{h}}\cdot\mathbf{p}_{1_T}\mathbf{p}_{2_T}^2\right)\frac{\bar{h}_1^{\perp f} h_{1T}^{\perp f}}{2M_1 M_2^2}\right]\Bigg\}. \tag{1.6}$$

Such a term depends explicitly on the Sivers function $f_{1T}^{\perp f}$, on the Transversity h_{1T}^f, and on the Boer-Mulders function $h_{1T}^{\perp f}$, where f is the parton flavour. These functions are weighted by $\sin(\varphi - \varphi_{S_2})$ and $\sin(\varphi+\varphi_{S_2})$, and selecting the proper angular dependence by mean of the corresponding experimental asymmetry, both the Boer-Mulders, the Sivers, and the Transversity functions can be accessed.

The Sivers function $f_{1T}^{\perp f}$ describes how the distribution of unpolarised quarks depends on the transverse polarisation of the parent hadron, and as such it contains informations on the orbital motion of hidden confined partons and on their spatial distribution [6]. This function can be accessed through its convolution with the unpolarised function f_1^f.

The Transversity function h_{1T}^f describes the density of transversely polarised quarks into a transversely polarised hadron. The Transversity can be accessed through its convolution with the Boer-Mulders function. In a single experimental scenario it is hence possible to access the BM function in the unpolarised case, and then use it to extract the Transversity in the single-spin case.

If both the beam and the target could be polarised, the differential cross section, after integrating upon dq_T, becomes [7]:

$$\frac{d\sigma^{\uparrow\uparrow}}{d\Omega dx_1 dx_2} = \frac{\alpha^2}{12Q^2}\Bigg[(1+\cos^2\vartheta)\sum_f e_f^2 \overline{f}_1^f(x_1) f_1^f(x_2) + \sin^2\vartheta\cos 2\varphi \frac{\tilde{\nu}(x_1,x_2)}{2} + |\mathbf{S}_{T1}||\mathbf{S}_{T2}|\sin^2\vartheta\cos(2\varphi-\varphi_{S_1}-\varphi_{S_2})\sum_f e_f^2 \overline{h}_{1T}^f(x_1) h_{1T}^f(x_2) + (1\leftrightarrow 2)\Bigg], \tag{1.7}$$

where the h_{1T}^f function can be directly accessed.

Three experimental asymmetries can thus be defined:

- $A^{\cos 2\varphi}$ for the unpolarised case;
- $A^{\sin(\varphi-\varphi_{S_2})}$, and $A^{\sin(\varphi+\varphi_{S_2})}$ for the single polarised case;
- $A^{\cos(2\varphi-\varphi_{S_1}-\varphi_{S_2})}$ for the double polarised case.

The unpolarised asymmetry can be obtained considering for each x_p bin events showing positive (U) and negative(D) values of $\cos 2\varphi$, the resulting asymmetry being $A^{\cos 2\varphi} = (U-D)/(U+D)$. The single- and double-spin asymmetries can be obtained in similar ways.

To perform a proper experimental investigation of such asymmetries one of the most relevant issues is the correct choice of the center of mass energy. In fact, at RHIC energies (p-p scattering at $\sqrt{s} \approx 200$ GeV) one can access TMD's mostly related to the sea quarks, leading hence to small expectations for the above described asymmetries. In the FAIR experimental scenario, that will be set at Darmstadt, Germany, such an investigation could be performed at a lower energy range and making use of antiproton beams: the valence quark's TMD's could hence be accessed. Two experiments have been proposed in such a scenario: the PANDA experiment [8] will access the energy region up to $s \approx 30$ GeV^2, and the PAX experiment up to $s \approx 200$ GeV^2 [9]. The key issue is making use of antiproton beams: each valence quark can thus contribute to the DY diagram. The PANDA experiment will investigate the unpolarised and, possibly, the single-polarised cases. The PAX Collaboration is planning to study the single-polarised and, if antiproton could be significantly polarised, the double-polarised scenarios.

2. PANDA Experimental Setup

The PANDA Collaboration [1, 8, 10] proposed to build a state-of-the-art universal detector for strong interaction studies hosted at the High-Energy Storage Ring (HESR) in the foreseen international FAIR facility in Darmstadt. The detector is designed to take advantage of the extraordinary physics potential which will be available utilizing high intensity, phase space cooled antiproton beams.

The collaboration is planning to exploit the antiproton beams provided by the new FAIR facility in a momentum range of $1.5 \div 15$ GeV/c in order to address fundamental questions on QCD. The physics program is intensively described in this volume by Tobias Stockmanns. The PANDA spectrometer allows for the study of electromagnetic processes as well. The foreseen luminosity (up to $2{\cdot}10^{32}$ cm^{-2}s^{-1}) will give access to processes like the Drell-Yan production of muon pairs.

The detector consists of two spectrometers. A target spectrometer (TS) surrounds the interaction region, and a forward spectrometer with a second magnet provides angular coverage for the most forward angles. The basic concept of the target spectrometer is a shell-like arrangement of various detector systems surrounding the interaction point inside the field of a large solenoid. The forward spectrometer covers the gap of detector acceptance in the forward region. The spectrometer apparatus is shown in Fig. 3.

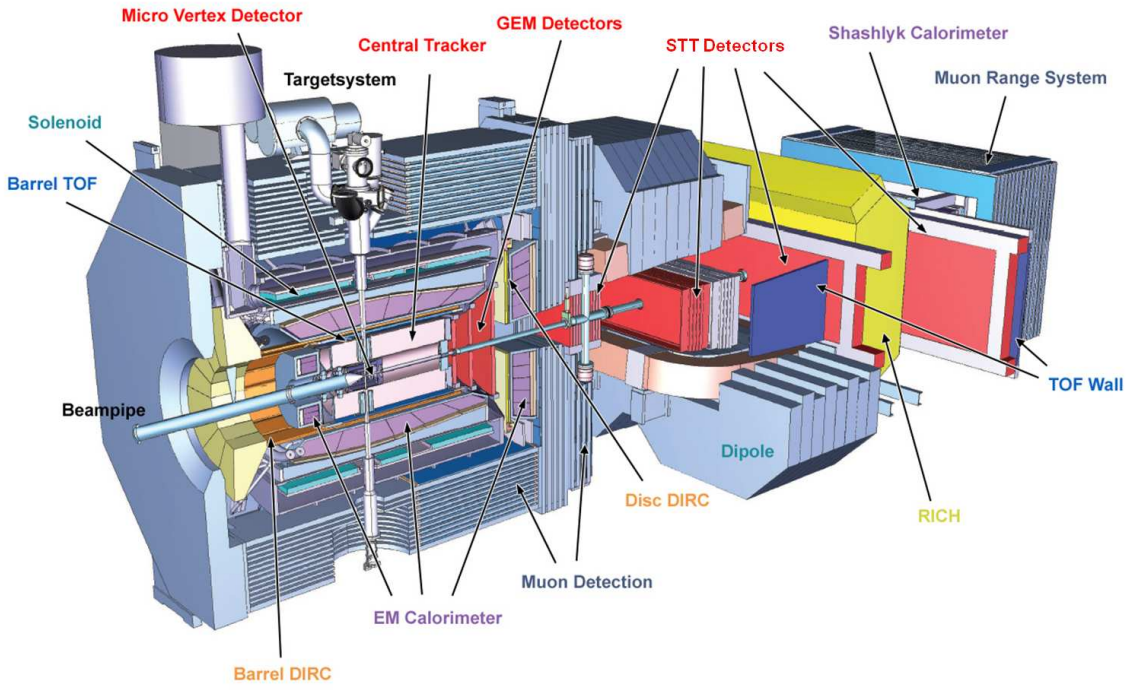

Figure 3: *Setup of the PANDA detector (3D view).*

The target spectrometer (TS) is an azimuthally symmetric system of detectors mostly contained inside the superconducting solenoid, including the muon counters (MUO) in between the magnet return yoke, and the forward end cap which may be situated just behind the magnet. This sector of PANDA spectrometer detects all those particles emitted at laboratory angles greater than 5° and 10°, in vertical and horizontal planes respectively, and lower than 140°. No particle detection is foreseen in the very backward region of 170°-180°. A silicon micro-vertex detector (MVD) surrounds the interaction volume. For a second tracking detector, two options are currently under investigation: or 12 straw tubes trackers (STT) double layers, or a time projection chamber (TPC). Particle identification is performed by the detection of the internally reflected Cherenkov light (DIRC) by mean of two detectors: one along the barrel (DIRC) and one in the endcap region (forward DIRC). The forward region is covered by three sets of gas electron multiplier (GEM). The inner detectors are surrounded by an electromagnetic calorimeter (EMC). Time-of-flight (TOF) counters provide the identification of the particles with momenta lower then 5 GeV/c. For the more forward directed particles the tracking is provided by MVD and GEMs. The muon counters (MUO), located within the segmented iron, are composed of Iarocci tubes (mini drift tubes

or MDT) in which the stainless steel cover is replaced by fiberglass strip boards (STRIP), which, collecting the induced charge, allow for the read out of the second coordinate. The MUO system will be optimized for the DY events reconstruction.

The current design of the forward spectrometer (FS) includes a 1 m gap dipole and tracking with straw tube trackers (STT). Photons are detected by a shashlyk-tipe calorimeter consisting of lead-scintillators sandwiches (EMC). The particle identification is provided by ring-imaging Cherenkov (RICH) and time-of-flight counters (TOF). The other neutrals and charged particles showing momenta close to the beam momentum are detected in the muon counters (MUO).

3. Drell-Yan Events in PANDA

The Drell-Yan processes that will be considered in the PANDA experiment are reactions of the type $\bar{p}p \rightarrow l^+l^-X$, electromagnetic processes in which a quark from the proton and an antiquark from the antiproton are annihilating into a virtual photon (γ^*). The virtual photon decays then into a lepton-antilepton pair, $e^+ - e^-$ or $\mu^+ - \mu^-$. The number of $e^+ - e^-$ pair per event is supposed to be quite high, due not only to particle decays but also to the secondary interactions which can occur inside the spectrometer. In order to have a better identification of the Drell-Yan events, the decay channel $\mu^+ - \mu^-$ is preferred. In this scenario, at the maximum provided center of mass energy (s = 30 GeV^2) the expected cross section is of the order of $\sigma \sim 1$ nb.

The most relevant foreseen background consists of events of the type $\bar{p}p \rightarrow n(\pi^+\pi^-)\,X$, where n indicates the number of the $\pi^+\pi^-$ pairs. Primary pions can generate fake signal in the muon detector. Moreover, since muons and pions have an almost similar mass, in case of pion decays into muons inside our magnetic field, the tilt angle between the decay pion and the decaying muon momenta can be lower than 2°, thus preventing to disentangle the two particles. The cross section in the PANDA energy range for such processes is estimated to be of the order of $\sigma \sim$ 20-30 μb. A background rejection factor of the order of 10^7 is hence required.

Normally a Drell-Yan process is investigated in the so called "safe region", the dilepton mass range just above the J/ψ peak and showing no contribution from resonances. In fact in the resonances region, this process should be disadvantaged, and should have a lower cross section. Previous experiments of proton-antiproton annihilation and di-lepton production, as E866 at Fermilab [11] or NA51 at CERN [12], have shown as the "safe region" is characterised by a dilepton mass ranging from 4 to 9 GeV/c^2. Unfortunately this region is characterised by an extremely low cross section. An alternate region characterised by a dilepton mass ranging from 1.5 to 2.5 GeV/c^2 can be considered as a "safe region", since free from resonances: in such a region the cross section is expected to be larger, and probing such a dilepton mass region as well allows to investigate larger kinematic region. The phase space plot in Fig. 4 reports the scatter plot of the longitudinal momentum fractions (x_1, x_2) of the two partons taking part in the annihilation. We can also define the variables $x_F = x_1 - x_2$ and $\tau = x_1 \cdot x_2$; the dashed diagonal lines and the dashed hyperbolae in the plot correspond to constant x_F and τ values, respectively. For dilepton masses between 4 and 9 GeV/c^2 we can access only the small area above the upper hyperbolae line. On the contrary to consider the dilepton mass region 1.5 $\div$ 2.5 GeV/c^2 gives access to the kinematic region limited by the double hyperbolae lines, straight and dashed, in the middle of the plot in the region 0.05 <

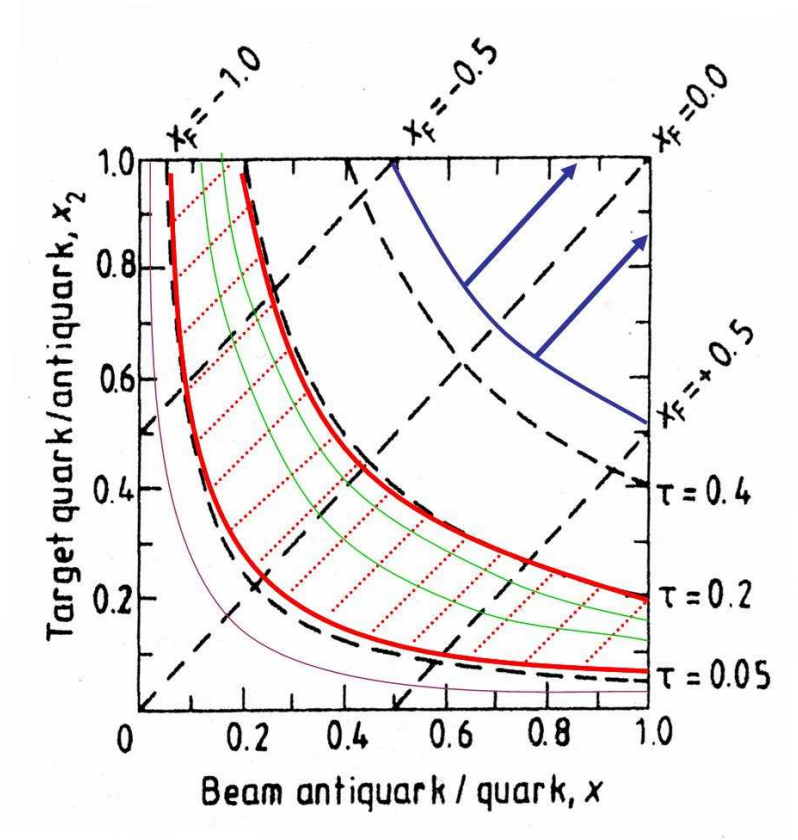

Figure 4: *Phase space plot for the Drell-Yan process with respect to $x_{1,2}$, the longitudinal momentum fractions of the parton$_{1,2}$ taking part to the annihilation in the DY process. Hyperbolae define the kinematic regions accessible at a given center of mass range.*

$\tau < 0.2$. This area corresponds also to the region of interest for PAX, limited inside the two tiny hyperbolae lines. Simulations show as events accumulate at lower τ values.

The Drell-Yan AB (DY_AB4) [13] event generator, developed for the PANDA collaboration by Prof. A. Bianconi, Università degli Studi di Brescia, Italy, is specifically intended for Drell-Yan (DY) studies, since it generates DY muon pairs in $\bar{p}$ and π^- interactions with unpolarized and polarized nuclear targets. The Drell-Yan production cross section is taken from experimental data [14, 15]. The events are sorted by a flat distribution of the variables x_1, x_2, P_T, ϑ, φ and φ_S and then accepted or rejected according to a cross section defined as:

$$\frac{d\sigma}{dx_1 dx_2 dP_T d\Omega} = \frac{K}{S} \cdot S(x_1, x_2) \cdot S'(P_T) \cdot A(\vartheta, \varphi, \varphi_S), \tag{3.1}$$

where x_1 and x_2 are the projections of the quark momentum (p_q) of the beam and of the target respectively on the momentum of the parent hadron (p_h); P_T is the transverse momentum of one hadron with respect to the other in the hadron center of mass frame (influencing the phase space distribution [16]); ϑ, φ and φ_S are the angular variables defined in the Collins-Soper frame (the virtual photon rest frame) shown in Fig. 2; S is the center of mass squared energy; A is the Collins-

Soper frame angular asymmetry of the form 1+....., where the corrections to "1" are within 10% [13].

The generator adopted for these simulations is an evolution of the one developed by A. Bianconi, in which the Sivers and the Collins effects are also taken into account. A full description of the generator can be found in [14, 15, 17]. The code provides as outputs the μ^+ and μ^- energy, and theta and phi variables.

This is the very same generator used by the COMPASS [18] Collaboration to perform the feasability studies for their future $\pi^- - N$ measurements.

Two million events were simulated. Of the generated events, 14.28% fall within the dilepton invariant mass region ranging from 1.5 to 2.5 GeV/c^2 ($\sigma^0 \sim 0.8$ nb), while only 35 events showed a dilepton mass in the $4 \div 9$ GeV/c^2 range ($\sigma^0 \sim 0.4$ pb).

4. Simulation Properties

The PandaRoot software framework [19] is now the official framework of the PANDA Collaboration. It is based on ROOT and Virtual Monte-Carlo. Due to its complexity, and its earlier stage, it is constantly developed and hence often modified. A stable version of such software framework was needed, in order to check the different effects of the setups and the possibilities we are investigating. Moreover, we wanted to perform a deep investigation of the direct Geant4 simulation software without including effects arising from other routines, as the Virtual Monte-Carlo ones.

We hence decided to freeze the official PANDA software release, and to develop our own simulation software. The simulation framework used to perform our studies is MISS (Muon Independent Simulation Software). It is a pure Geant4 simulation software and the package ROOT was used for the storage and the plots preparation only. We included in the simulated geometry only the target spectrometer (TS). The design of the implemented magnet corresponds to the one provided in the november 2007 release of the official PANDA software, and for the magnetic field we implemented the design provided by the Genova group (Italy). Layers of muon detectors were placed every 2 cm of iron in the yoke of the solenoidal magnet, and those sensible volumes were filled with a mixture of Ar+CO_2.

The events for the foreseen background processes were generated by the PYTHIA 8 [20] software, completely written in C++ language. As already explained in par. 3, the main background is expected to arise from processes as $\bar{p}p \rightarrow n(\pi^+\pi^-)\,X$. The background was classified into two main sets: primary and secondary. The primary background includes primary pions, created at the interaction point, and the secondary muons, coming from the decay of the primary pions. The secondary background consists of secondary pions and secondary muons, from the decay of the secondary pions.

5. Analysis and Results

Our simulations showed as the Drell-Yan events are boosted to the forward angles. Most of the signal consists of two muons which should cross the endcap of the TS. The contributions from the forward spectrometer region are hence expected not to be negligible. A small contribution to the signal from muon pairs in which one muon is crossing the barrel side of the TS and the other

one the endcap of the TS has been observed as well. For a better explanation of the obtained results refer to [21].

An important effort was devoted to identify the cuts needed for the background rejection, and their effects on both the signal and the background. Table 1 reports the effects of the different investigated cuts on the signal, and on the primary (Prim) and the secondary (Sec) background. The

	Iron	Hit	q_T
Signal	Linear	30%	65%
Prim	Linear	10^3	10^4
Sec	Negligible	10^4	$> 5{\cdot}10^6$

Table 1: Cuts and rejection on signal and primary and secondary background.

iron planes (Iron) between two muon detector layers do not provide by themselves the requested rejection factor of $\sim 10^7$; a kinematic selection of the events' sample is hence needed. For this reason, we have to introduce some kinematic cuts into our sample. First, the candidate muon tracks should give a signal at least in one of the first two muon detector layers (Hit), in order to exclude those muons produced inside the iron yoke. Even if such a cut rejects $\sim$ 30% of the signal, it also selects muon pairs with enough energy to pass through all the planes of the muon detector without being stopped in between. A further kinematic cut is performed on the tranverse momentum of the muon pair (q_T). With these cuts, it is possible to reconstruct $\sim$ 35% of the signal, yet achieving for the secondary background a rejection factor larger than $5{\cdot}10^6$. For a more precise estimation of the secondary background rejection new simulations, where the number of the generated background events should be at least 2 orders of magnitude larger, are needed. On the other hand, the rejection of the primary background is still insufficient; the needed rejection value could be probably reached performing a kinematically constrained refit feeded with the candidate muon tracks. With the combined request for all the candidate tracks to be created in the target region, a proper primary background reduction is foreseen [21].

The simulated Drell-Yan asymmetries for the unpolarised and single-polarised cases are presented in Fig. 5-7 for two different muon pair transverse momenta intervals: $1 \leq q_T \leq 2$ GeV/c (light dots), and $2 \leq q_T \leq 3$ GeV/c (dark dots). There is no x_p dependence in the generated events for these simulations, the plots in Fig. 5-7 just showing part of the accessible kinematic region at this center of mass energy and in this di-lepton mass range. Fig. 5 shows for the unpolarised case the simulated experimental asymmetry related to the $\cos(2\varphi)$ term, plotted as a function of the longitudinal momentum fraction of the hadronic probe (x_p). Fig. 6 and 7 show for the single-polarised case the simulated experimental asymmetries related to the $\sin(\varphi+\varphi_S)$ and $\sin(\varphi-\varphi_S)$ angular terms, again plotted as functions of x_p. Those results were obtained making use of 500000 simulated events. The plots are not yet acceptance and efficiency corrected, although these corrections are crucial for our studies.

In the unpolarised case the asymmetries are expected to be small but not negligible; it should anyhow be possible to study the asymmetry dependency on the transverse momentum of the lepton pair. The investigation of a possible inversion of such dependence, making use of a scan on the full transverse momentum range, would allow to probe the balance between soft and hard processes for

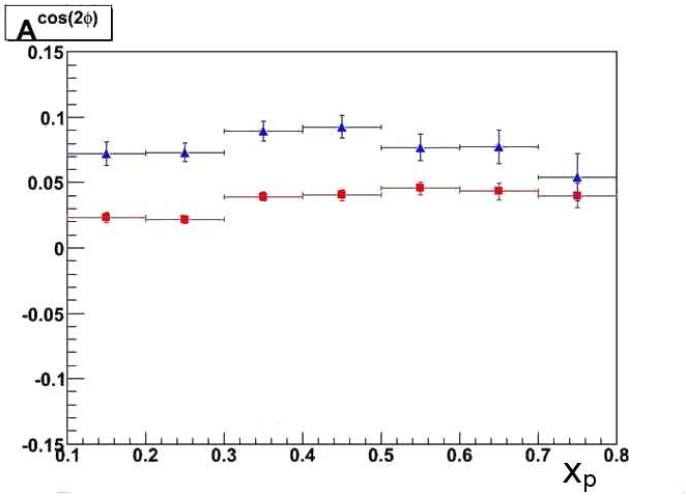

Figure 5: *Simulated experimental asymmetry related to the* $\cos 2\varphi$ *term, plotted as a function of* x_p*, longitudinal momentum fraction of the hadronic probe.*

DY production of lepton pairs in the PANDA energy range.

In the single-polarised case, the simulated distributions show how, according to the considered generator, an investigation of the possible dependence of the experimental asymmetries on the transverse momentum of the lepton pair could be more difficult or eventually impossible, according to which experimental asymmetry is considered.

Further studies evaluating the expected experimental errors from asymmetry measurements have been performed as well and are reported in details in [21].

The investigations reported in the present paper will be soon performed in the official PandaRoot framework that has in the meantime reached a much more mature stage. The achieved rejections factors quoted above can hence be counterchecked, and a complete kinematic event selection scheme can be developed and validated. A significantly larger statistics (10^8 events) is also needed.

6. Aknowledgements

This work was supported in part by Università degli Studi di Torino, Regione Piemonte, and INFN Torino.

References

[1] W. Erni, et al., *Physics Performance Report for: PANDA, Strong Interaction Studies with Antiproton*, (2009)

[2] C. Bourrely and J. Soffer, *Do we understand the single-spin asymmetry for* π^0 *inclusive production in pp collisions?*, Eur. Phys. J. **C36**, 371 (2004)

[3] J. C. Collins and D. E. Soper, *Angular distribution of dileptons in high-energy hadron collisions*, Phys. Rev. **D16**, 2219 (1977)

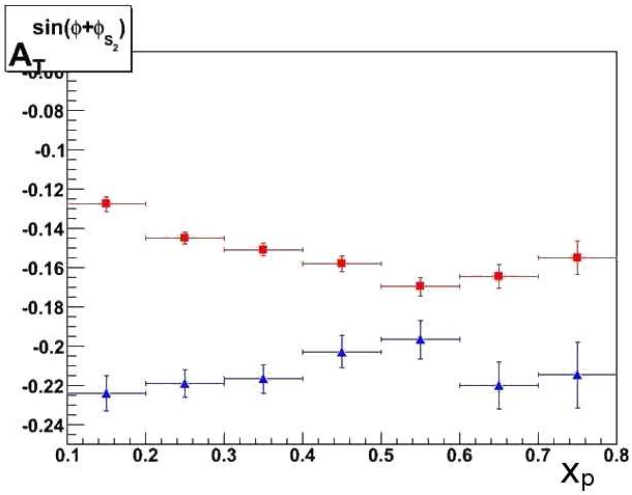

Figure 6: *Simulated experimental asymmetry related to the* $\sin(\varphi + \varphi_{S_2})$ *term, plotted as a function of* x_p*, longitudinal momentum fraction of the hadronic probe.*

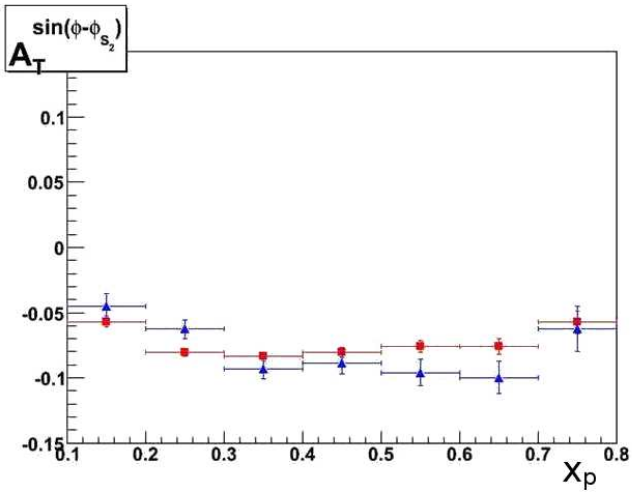

Figure 7: *Simulated experimental asymmetry related to the* $\sin(\varphi - \varphi_{S_2})$ *term, plotted as a function of* x_p*, longitudinal momentum fraction of the hadronic probe.*

[4] J. C. Collins, *Leading-twist Single-transverse-spin asymmetries: Drell-Yan and Deep-Inelastic Scattering*, Phys. Lett. **B 536**:43-48 (2002)

[5] J. C. Collins and D. E. Soper, *Parton distribution and decay functions*, Nucl. Phys. **B 194**, 445 (1982)

[6] M. Burkardt and D. S. Hwang, *Sivers effect and generalized parton distributions in impact parameter space*, Phys. Rev. **D69**, 074032 (2004)

[7] R. D. Tangerman, and P. J. Mulders, *Intrinsic transverse momentum and the polarized Drell-Yan process*, Phys. Rev. **D51**, 3357 (1995)

[8] M. Kotulla, et al., *Letter of Intent for: PANDA, Strong Interaction Studies with Antiproton*, (2004)

[9] V. Barone, et al., *Technical Proposal for PAX*, (2005)

[10] M. Kotulla, et al., *PANDA Technical Progress Report, Strong Interaction Studies with Antiproton*, (2005)

[11] P.L. McGaughey, et al., *High-Energy Hadron-Induced Dilepton Production from Nucleons and Nuclei*, Ann. Rev. Nucl. Part. Sci. **49**, 217-253 (1999)

[12] A. Baldit, et al., *Study of the isospin symmetry breaking in the light quark sea of the nucleon from the Drell-Yan process*, Phys. Lett. **B 332**, 244 (1994)

[13] A. Bianconi, *Monte Carlo Event Generator DY_AB4 for Drell-Yan Events with Dimuon Production in Antiproton and Negative Pion Collisions with Molecular Targets*, Panda Internal Note, (2006)

[14] A. Bianconi and M. Radici, *Monte Carlo simulation of events with Drell-Yan lepton pairs from antiproton-proton collisions*, Phys. Rev. **D71**, 074014 (2005)

[15] A. Bianconi and M. Radici, *Monte Carlo simulation of events with Drell-Yan lepton pairs from antiproton-proton collisions: The fully polarized case*, Phys. Rev. **D72**, 074013 (2005)

[16] O. Linnyk, *Quark Off-Shellness effect on parton distributions*, WiKu Editions, Duisburg-Köln (2006)

[17] A. Bianconi, *A scheme for fast exploratory simulation of azimuthal asymmetries in Drell-Yan experiments at intermediate energies. The DY_AB Monte Carlo event generator*, Nucl. Inst. Meth. A593:562-571 (2008)

[18] G. Baum et al., *COMPASS: A proposal for a COmmon Muon and Proton Apparatus for Structure and Spectroscopy*, CERN/SPSLC 96-14, SPSC/P 297 (1996)

[19] S. Spataro, et al., *Simulation and event reconstruction inside the PandaRoot framework*, J. Phys.: Conf. Ser. **119** 032035 (2008)

[20] http://home.thep.lu.se/ torbjorn/Pythia.html

[21] M. Destefanis, et al., *Azimuthal asymmetries for Drell-Yan di-muon production in the PANDA scenario*, Proceedings of the XLVII International Winter Meeting on Nuclear Physics, 26-30 January 2009, Vol.99 Italian Physical Society, Bologna (2010)